Inorg. Chem. **2005**, *44*, 2803–2814

Six-Coordinate Titanium Complexes of a Tripodal Aminetris(phenoxide) Ligand: Synthesis, Structure, and Dynamics

Kevin C. Fortner, Julian P. Bigi, and Seth N. Brown*

Department of Chemistry and Biochemistry, 251 Nieuwland Science Hall, University of Notre Dame, Notre Dame, Indiana 46556-5670

Received November 12, 2004

The five-coordinate titanium(IV) alkoxide LTi(O^{t}Bu) (LH_3 = tris(2-hydroxy-3,5-di-*tert*-butylbenzyl)amine) is protonolyzed readily by the conjugate acids of monoanionic bidentate ligands, both symmetrical (tropolone, acetylacetone, di-*p*-toluoylmethane) and unsymmetrical (8-hydroxyquinoline, salicylaldehyde, 2,6-diformyl-*p*-cresol, anthrarufin). The geometry of these complexes, which is pseudo-octahedral with the tripodal ligand adopting a chiral, propeller-like conformation, has been confirmed in four cases by X-ray crystallography. Variable-temperature NMR spectroscopy indicates that the six-coordinate complexes undergo two dynamic processes. First, the ligands undergo a twisting motion that results in racemization, a process which is over 10^4 times faster than in five-coordinate complexes. The rate acceleration upon binding of an equatorial ligand is ascribed to steric repulsions with one of the *cis* phenoxides; the dynamics of a binuclear dibenzyl phosphate-bridged compound, which has a unique conformation of the tripodal ligand, indicates that flexing the *cis* phenoxide is the rate-limiting step in racemization. Second, the complexes undergo a process that interchanges the inequivalent arms of the tripodal ligand. This process involves a trigonal twist that shifts the bidentate ligand between clefts in the tripod. The intermediate geometry in the reaction appears to be a transition state and not a long-lived intermediate, as judged from the relative rates of interconversion of tripod arms and chelate ends in the ditoluoylmethane complex. Tripod arm interchange takes place without partial dissociation of the bidentate chelate, a reaction that has been observed on a slower time scale in one case.

Introduction

Tripodal, trianionic ligands such as trialkoxyamines[1] and triamidoamines[2] play important roles in inorganic chemistry and have been used to stabilize unusual coordination geometries,[3] unusual inorganic functionalities,[4] and catalytically active species.[5] While complexes of such tripodal ligands are known in a variety of coordination numbers and geometries, five-coordinate trigonal bipyramidal complexes are by far the most commonly observed. However, the structure and dynamics of higher-coordinate species are of interest as potential models for intermediates in catalytic reactions of such tripodal complexes.

Ligands derived from deprotonation of derivatives of tris(2-hydroxybenzyl)amine are a relatively new class of tri-

* Author to whom correspondence should be addressed. E-mail: seth.n.brown.114@nd.edu.

(1) (a) Verkade, J. G. *Coord. Chem. Rev.* **1994**, *137*, 233−295. (b) Verkade, J. G. *Acc. Chem. Res.* **1993**, *26*, 483−489.
(2) Schrock, R. R. *Acc. Chem. Res.* **1997**, *30*, 9−16.
(3) (a) Cummins, C. C.; Lee, J.; Schrock, R. R.; Davis, W. M. *Angew. Chem., Int. Ed. Engl.* **1992**, *31*, 1501−1503. (b) Pinkas, J.; Wang, T. L.; Jacobson, R. A.; Verkade, J. G. *Inorg. Chem.* **1994**, *33*, 4202−4210. (c) Ray, M.; Golombek, A. P.; Hendrich, M. P.; Young, V. G.; Borovik, A. S. *J. Am. Chem. Soc.* **1996**, *118*, 6084−6085. (d) Rosenberger, C.; Schrock, R. R.; Davis, W. M. *Inorg. Chem.* **1997**, *36*, 123−125. (e) Roussel, P.; Alcock, N. W.; Scott, P. *Chem. Commun.* **1998**, 801−802. (f) Ray, M.; Hammes, B. S.; Yap, G. P. A.; Rheingold, A. L.; Borovik, A. S. *Inorg. Chem.* **1998**, *37*, 1527−1532. (g) Schneider, S.; Filippou, A. C. *Inorg. Chem.* **2001**, *40*, 4674−4677. (h) Filippou, A. C.; Schneider, S.; Schnakenburg, G. *Inorg. Chem.* **2003**, *42*, 6974−6976.
(4) (a) Cummins, C. C.; Schrock, R. R.; Davis, W. M. *Angew. Chem., Int. Ed. Engl.* **1993**, *32*, 756−759. (b) Christou, V.; Arnold, J. *Angew. Chem., Int. Ed. Engl.* **1993**, *32*, 1450−1452. (c) Cummins, C. C.; Schrock, R. R.; Davis, W. M. *Inorg. Chem.* **1994**, *33*, 1448−1457. (d) Zanetti, N. C.; Schrock, R. R.; Davis, W. M. *Angew. Chem., Int. Ed. Engl.* **1995**, *34*, 2044−2046. (e) Mösch-Zanetti, N. C.; Schrock, R. R.; Davis, W. M.; Wanninger, K.; Seidel, S. W.; O'Donoghue, M. B. *J. Am. Chem. Soc.* **1997**, *119*, 11037−11048.
(5) (a) Yandulov, D. V.; Schrock, R. R. *Science* **2003**, *301*, 76−78. (b) Ritleng, V.; Yandulov, D. V.; Weare, W. W.; Schrock, R. R.; Hock, A. S.; Davis, W. M. *J. Am. Chem. Soc.* **2004**, *126*, 6150−6163. (c) DiFuria, F.; Licini, G.; Modena, G.; Motterle, R.; Nugent, W. A. *J. Org. Chem.* **1996**, *61*, 5175−5177. (d) Bonchio, M.; Calloni, S.; DiFuria, F.; Licini, G.; Modena, G.; Moro, S.; Nugent, W. A. *J. Am. Chem. Soc.* **1997**, *119*, 6935−6936. (e) Nugent, W. A. *J. Am. Chem. Soc.* **1992**, *114*, 2768−2769. (f) McCleland, B. W.; Nugent, W. A.; Finn, M. G. *J. Org. Chem.* **1998**, *63*, 6656−6666. (g) Nugent, W. A. *J. Am. Chem. Soc.* **1998**, *120*, 7139−7140. (h) Kim, Y.; Hong, E.; Lee, M. H.; Kim, J.; Han, Y.; Do, Y. *Organometallics* **1999**, *18*, 36−39.

10.1021/ic048403d CCC: $30.25 © 2005 American Chemical Society
Published on Web 03/22/2005

anionic, tripodal ligands that have recently been explored as supporting ligands for early[6−8] and later[9] transition metals as well as main group elements.[10] The ligands are attractive in that they are sterically and electronically tunable by judicious choice of substituents on the aryl rings and appear to lend good stability to their complexes. For example, titanium(IV) complexes $[N(CH_2C_6H_2\text{-}3,5\text{-}{}^tBu_2\text{-}2\text{-}O)_3]Ti(OR)$ (LTi[OR]) have been observed to be highly resistant to hydrolysis.[11] Here, we describe the preparation of a variety of six-coordinate complexes of the LTi^{IV} fragment containing bidentate, monoanionic chelates. Six-coordination is readily achieved in these complexes, and their geometries are relatively undistorted octahedra. The complexes do exhibit a rich variety of fluxional behaviors, including ligand conformational changes, configurational changes about the metal, and partial dissociation of the bidentate ligand.

Experimental Section

General Procedures. Unless otherwise noted, all procedures were carried out on the benchtop. CD_2Cl_2 used in variable-temperature NMR experiments was dried over molecular sieves, followed by CaH_2, and stored in an inert-atmosphere drybox before use. Tetrahydrofuran was dried over sodium benzophenone ketyl. 2,6-Diformyl-*p*-cresol was prepared by the MnO_2 oxidation of commercially available 2,6-bis(hydroxymethyl)-*p*-cresol as described by Xie et al.[12] LTi(O^{t}Bu) (LH_3 = tris(2-hydroxy-3,5-di-*tert*-butylbenzyl)amine) was prepared as previously described.[11] All other reagents and solvents were commercially available and used as received. ^{1}H and ^{13}C{^{1}H} NMR spectra (referenced to tetramethylsilane) were obtained on a Varian VXR-300 or VXR-500 spectrometer and were recorded at room temperature (20 °C) unless otherwise indicated. ^{31}P NMR spectra were referenced to external 85% H_3PO_4. IR spectra were measured as evaporated films on a Perkin-Elmer PARAGON 1000 FT-IR spectrometer and are reported in wavenumbers (cm^{-1}). Fast atom bombardment (FAB) mass spectra were obtained on a JEOL LMS-AX505HA mass spectrometer using 3-nitrobenzyl alcohol as a matrix. Peaks reported are the mass number of the most intense peak of isotope envelopes; in all cases, isotope patterns were in agreement with values calculated from the molecular formulas. For EI mass spectral analysis, a JEOL GCmate spectrometer using EI ionization mode was employed. Elemental analyses were performed by M-H-W Laboratories (Phoenix, AZ).

All of the LTi complexes have the following IR peaks, within 3 cm^{-1}: 2954 (s), 2904 (m), 2868 (m), 1474 (m), 1444 (m), 1412 (w), 1361 (m), 1306 (w), 1260 (s), 1240 (m), 1204 (w), 1171 (w), 1128 (w), 915 (w), 873 (w), 852 (m), 811 (w), 758 (m). Only unique peaks are reported for the individual compounds.

[Nitrilotris(3,5-di-*tert*-butyl-2-cresolato)](tropolonato)titanium(IV), LTi(trop). To a solution of 300 mg of LTi(O^{t}Bu) (0.380 mmol) in 20 mL of benzene was added tropolone (48 mg, 0.392 mmol, 1.03 equiv), causing an immediate color change from yellow to orange. The solution was stirred for 1 h, and the solvent and ^{t}BuOH were removed on a rotary evaporator, leaving behind an orange oil. The oil was dissolved in a minimum of benzene (~3 mL), and 30 mL of CH_3CN was added to the solution. The CH_3CN/benzene solution was mixed thoroughly and was placed in a refrigerator. Crystallization was complete within 24 h. The orange crystals were suction-filtered on a glass frit, washed with CH_3CN (3 × 5 mL), and air-dried. Yield: 306 mg (96%). ^{1}H NMR (C_6D_6): δ 1.37 (s, 27H, ^{t}Bu), 1.55 (s, 27H, ^{t}Bu), 3.82 (br s, 6H, NC*H*$_2$Ar), 6.09 (t, 9.8 Hz, 1H, tropolone 5-H), 6.41 (dd, 11.1, 9.8 Hz, 2H, tropolone 4,6-H), 6.62 (d, 11.1 Hz, 2H, tropolone 3, 7-H), 6.97 (d, 2.5 Hz, 3H, Ar*H*), 7.47 (d, 2.5 Hz, 3H, Ar*H*). ^{13}C-{^{1}H} NMR ($CDCl_3$): δ 30.24, 31.93, 34.40, 35.08, 62.08, 123.44, 123.94, 124.56, 125.69, 128.33, 135.00, 139.06, 141.98, 159.36, 182.16. IR: 1596 (m), 1574 (w), 1522 (s), 1435 (s), 1332 (m), 1073 (w), 968 (w), 714 (w). FAB-MS: 837 (M^+). Anal. Calcd for $C_{52}H_{71}NO_5Ti$: C, 74.53; H, 8.54; N, 1.67. Found: C, 74.74; H, 8.38; N, 1.76.

[Nitrilotris(3,5-di-*tert*-butyl-2-cresolato)](acetylacetonato)titanium(IV), LTi(acac), was prepared by the same method as the tropolonate, using 300 mg of LTi(O^{t}Bu) (0.380 mmol) and 0.100 mL (0.974 mmol, 2.6 equiv) of 2,4-pentanedione. The yield of orange LTi(acac) was 291 mg (94%). ^{1}H NMR ($CDCl_3$): δ 1.25 (s, 27H, ^{t}Bu), 1.31 (s, 27H, ^{t}Bu), 1.84 (s, 6H, acac C*H*$_3$), 3.84 (br s, 6H, NC*H*$_2$Ar), 5.51 (s, 1H, acac C*H*), 6.91 (d, 2.1 Hz, 3H, Ar*H*), 7.13 (d, 2.1 Hz, 3H, Ar*H*). ^{13}C{^{1}H} NMR ($CDCl_3$): δ 26.16, 30.35, 31.99, 34.42, 35.10, 62.40, 104.80, 123.40, 123.85, 125.02, 134.86, 141.00, 159.45, 190.36. IR: 1594 (m), 1520 (m), 1026 (w). FAB-MS: 815 (M^+). Anal. Calcd for $C_{50}H_{73}NO_5Ti$: C, 73.60; H, 9.02; N, 1.72. Found: C, 73.73; H, 8.99; N, 1.73.

Di-*p*-toluoylmethane (Hdtm). In the drybox, to a solution of 0.465 g of 4′-methylacetophenone (Aldrich, 3.46 mmol) in 2 mL of dry THF in a 20-mL screw-cap vial was added a solution of 1.215 g of lithium bis(trimethylsilyl)amide (Aldrich, 7.26 mmol, 2.1 equiv) in 10 mL of THF. To this solution was added, dropwise over 5 min with occasional swirling, a solution of 0.499 g of *p*-toluoyl chloride (Aldrich, 3.22 mmol, 0.93 equiv) in 2 mL of THF. The reaction mixture gets very hot, and near the end of the addition Li(dtm) begins to precipitate as an off-white solid. The vial was capped securely and allowed to stand overnight at room temperature. The reaction mixture was then opened to the air and suction filtered on a glass frit, and the precipitate was washed with 2 × 5 mL Et_2O. The filtrate was reserved, and the precipitate was partitioned between 1 M HCl (30 mL) and Et_2O (40 mL). The aqueous layer was discarded, and the organic layer (including a small amount of suspended solids) was treated with an additional 20 mL each of aqueous HCl and Et_2O. The organic layer was washed with 20 mL of water, dried over $MgSO_4$, and evaporated to give 0.391 g of di-*p*-toluoylmethane, mp 125−126.5° (lit.[13] 123.5−125°). A second crop of 0.189 g was obtained by evaporating the filtrate to dryness and working up in the same manner; combined yield, 0.579 g, 71% based on toluoyl chloride. The ^{1}H NMR spectrum in $CDCl_3$ indicates that the compound exists

(6) Kol, M.; Shamis, M.; Goldberg, I.; Goldschmidt, Z.; Alfi, S.; Hayut-Salant, E. *Inorg. Chem. Commun.* **2001**, *4*, 177−179.

(7) (a) Michalczyk, L.; de Gala, S.; Bruno, J. W. *Organometallics* **2001**, *20*, 5547−5556. (b) Kim, Y.; Verkade, J. G. *Organometallics* **2002**, *21*, 2395−2399. (c) Bull, S. D.; Davidson, M. G.; Johnson, A. L.; Robinson, D. E. J. E.; Mahon, M. F. *Chem. Commun.* **2003**, 1750−1751. (d) Davidson, M. G.; Doherty, C. L.; Johnson, A. L.; Mahon, M. F. *Chem. Commun.* **2003**, 1832−1833.

(8) (a) Groysman, S.; Segal, S.; Shamis, M.; Goldberg, I.; Kol, M.; Goldschmidt, Z.; Hayut-Salant, E. *J. Chem. Soc., Dalton Trans.* **2002**, 3425−3426. (b) Kim, Y.; Kapoor, P. N.; Verkade, J. G. *Inorg. Chem.* **2002**, *41*, 4834−4838. (c) Groysman, S.; Goldberg, I.; Kol, M.; Goldschmidt, Z. *Organometallics* **2003**, *22*, 3793−3795.

(9) Hwang, J.; Govindaswamy, K.; Koch, S. A. *Chem. Commun.* **1998**, 1667−1668.

(10) Chandrasekaran, A.; Day, R. O.; Holmes, R. R. *J. Am. Chem. Soc.* **2000**, *122*, 1066−1072.

(11) Ugrinova, V.; Ellis, G. A.; Brown, S. N. *Chem. Commun.* **2004**, 468−469.

(12) Xie, R. G.; Zhang, Z. J.; Yan, J. M.; Yuan, D. Q. *Synth. Commun.* **1994**, *24*, 53−58.

(13) Choshi, T.; Horimoto, S.; Wang, C. Y.; Nagase, H.; Ichikawa, M.; Sugino, E.; Hibino, S. *Chem. Pharm. Bull.* **1992**, *40*, 1047−1049.

exclusively as the *cis* enol: δ 2.43 (s, 6H, CH_3), 6.81 (s, 1H, =C−H), 7.29, 7.89 (d, 9 Hz, 4H each, Ar−H), 16.95 (v br s, 1H, O−H).

[Nitrilotris(3,5-di-*tert*-butyl-2-cresolato)](di-*p*-toluoylmethanato)titanium(IV), LTi(dtm), was prepared by the same method as LTi(trop) and LTi(acac), using 103 mg of LTi(O^{t}Bu) and 38.9 mg of Hdtm (0.154 mmol, 1.2 equiv). The yield of orange crystals was 84.5 mg (67%). ^{1}H NMR (CD_2Cl_2, 258 K; the molecule has $\sim C_s$ symmetry on the NMR time scale at this temperature): δ 1.08 (s, 18H, ^{t}Bu), 1.26 (s, 9H, ^{t}Bu), 1.27 (s, 18H, ^{t}Bu), 1.64 (s, 9H, ^{t}Bu), 2.28 (s, 3H, CH_3), 2.46 (s, 3H, CH_3), 3.60−4.20 (br, 6H, NCH_2), 6.86 (s, 1H, CH[COTol]$_2$), 7.01 (d, 8 Hz, 2H, tolyl ArH), 7.02 (d, 2 Hz, 2H, L ArH), 7.05 (d, 8 Hz, 2H, tolyl ArH), 7.07 (d, 2 Hz, 3H, L ArH), 7.29 (d, 2 Hz, 1H, L ArH), 7.35 (d, 8 Hz, 2H, tolyl ArH), 8.03 (d, 8 Hz, 2H, tolyl ArH). ^{13}C{^{1}H} NMR (CD_2Cl_2, 258 K): δ 21.69, 21.84, 29.52, 29.88, 31.71, 31.80, 34.38, 34.51, 34.80, 35.43, 60.92, 61.77, 97.76, 123.43, 123.65, 124.02, 124.30, 125.18, 126.52, 127.80, 128.03, 129.48, 129.73, 134.05, 134.47, 134.73, 135.63, 140.77, 141.97, 143.43, 143.69, 158.66 (br), 160.59, 181.33, 186.43. IR: 1609 (w), 1589 (m), 1548 (s), 1520 (s), 1489 (s), 1318 (m), 1184 (m), 1062 (m), 1018 (w), 784 (m), 694 (w), 634 (m), 603 (s). FAB-MS: 967 (M$^+$). Anal. Calcd for $C_{62}H_{81}NO_5Ti$: C, 76.91; H, 8.43; N, 1.45. Found: C, 77.12; H, 8.27; N, 1.52.

[Nitrilotris(3,5-di-*tert*-butyl-2-cresolato)](8-oxyquinolinato)titanium(IV), LTi(hq). To a solution of 200 mg of LTi(O^{t}Bu) (0.253 mmol) in 20 mL of benzene was added solid 8-hydroxyquinoline (50 mg, 0.342 mmol, 1.35 equiv). The solution was refluxed for 2 h, with the color changing from yellow to orange after a few minutes at reflux. The volatiles were removed on a rotary evaporator. The orange oil was redissolved in benzene (7 mL) and allowed to reflux for an additional hour to ensure that all of the LTi(O^{t}Bu) had reacted. The solvent was again evaporated, and the orange oil was dissolved in 50 mL of hexane and was washed with CH_3CN (3 × 20 mL) to remove unreacted 8-hydroxyquinoline. The hexane layer was placed on a rotary evaporator, and the solvent was removed to leave an orange solid. The solid was recrystallized by dissolving it in a minimum of benzene, and layering the solution with 20 mL of CH_3CN. Orange crystals, which were suitable for X-ray analysis, formed within 24 h. The crystals were filtered, washed with CH_3CN (3 × 5 mL), and air-dried on a glass frit to give 179 mg (82%) LTi(hq). ^{1}H NMR (CD_2Cl_2): δ 1.08 (s, 27H, ^{t}Bu), 1.28 (s, 27H, ^{t}Bu), 3.78 (br s, 6H, NCH_2Ar), 6.82 (dd, 4.8, 1.4 Hz, 1H, hq H-2), 6.92 (dd, 8.2, 4.8 Hz, 1H, hq H-3), 7.00 (dd, 7.8, 1.2 Hz, 1H, hq H-4), 7.06 (d, 2.5 Hz, 3H, ArH), 7.13 (d, 2.5 Hz, 3H, ArH), 7.16 (dd, 8.2, 1.2 Hz, 1H, hq H-5), 7.48 (dd, 8.2, 7.8 Hz, 1H, hq H-6), 8.02 (dd, 8.2, 1.4 Hz, 1H, hq H-7). ^{13}C{^{1}H} NMR (C_6D_6): δ 30.50, 32.35, 34.82, 35.61, 61.53, 113.24, 116.27, 120.84, 124.32, 124.66, 125.32, 129.97, 130.32, 136.61, 137.54, 141.96, 144.43, 144.51, 160.45, 162.35. IR: 1601 (w), 1580 (w), 1499 (m), 1470 (s), 1320 (w), 1106 (m), 822 (w), 784 (w), 744 (m), 635 (w). FAB-MS: 860 (M$^+$).

[Nitrilotris(3,5-di-*tert*-butyl-2-cresolato)](2-formylphenoxo)titanium(IV), LTi(sal), was prepared by the same method as the hydroxyquinolinate complex, using 200 mg of LTi(O^{t}Bu) (0.253 mmol) and 0.5 mL of salicylaldehyde (4.7 mmol, 19 equiv), yielding 184 mg (87%) of LTi(sal) as orange crystals. ^{1}H NMR (C_6D_6): δ 1.38 (s, 27H, ^{t}Bu), 1.48 (br, 27H, ^{t}Bu), 3.79 (br s, 6H, NCH_2Ar), 6.30 (ddd, 7.8, 7.0, 0.9 Hz, 1H, sal 4-H), 6.48 (dd, 7.8, 1.8 Hz, 1H, sal 3-H), 6.89 (dd, J = 8.5, 0.9 Hz, 1H, sal 6-H), 7.00 (d, 2.4 Hz, 3H, ArH), 7.04 (ddd, J = 8.5, 7.0, 1.8 Hz, 1H, sal 5-H), 7.46 (d, 2.4 Hz, 3H, ArH), 8.01 (s, 1H, CHO). ^{13}C{^{1}H} NMR (CD_2Cl_2): δ 30.12, 32.04, 34.73, 35.32, 61.86, 119.54, 120.28, 123.78, 124.68, 125.36, 125.43, 135.57, 136.55, 140.50, 141.89, 159.42, 167.75, 194.20. IR: 1631 (s), 1604 (w), 1543 (m), 1402 (w), 1146 (w), 906 (w), 790 (w). FAB-MS: 837 (M$^+$). Anal. Calcd for $C_{52}H_{71}NO_5Ti$: C, 74.53; H, 8.54; N, 1.67. Found: C, 74.75; H, 8.38; N, 1.70.

[Nitrilotris(3,5-di-*tert*-butyl-2-cresolato)](2,6-diformyl-*p*-cresolato)titanium (IV), LTi(dfc). To a solution of 200 mg of LTi(O^{t}Bu) (0.253 mmol) in 20 mL of dichloromethane was added 2,6-diformyl-*p*-cresol (45 mg, 0.274 mmol, 1.1 equiv). The solution was refluxed for 4 h, with the color of the solution changing from yellow to orange after a few minutes at reflux. The solvent and ^{t}BuOH were removed on a rotary evaporator to leave behind an orange solid. The solid was recrystallized by dissolving it in a minimum of CH_2Cl_2 and layering the solution with 20 mL of CH_3CN. Reddish-orange crystals of LTi(dfc), which were suitable for X-ray analysis, formed within 24 h. The crystals were filtered, washed with CH_3CN (3 × 5 mL), and air-dried on a glass frit. Yield: 210 mg (94%). ^{1}H NMR (CD_2Cl_2, 273 K; the molecule has $\sim C_s$ symmetry on the NMR time scale at this temperature): δ 1.01 (s, 18H, ^{t}Bu), 1.25 (s, 27H, ^{t}Bu), 1.57 (s, 9H, ^{t}Bu), 3.72 (broad s, 2H, NCH_2Ar trans to CHO), 3.75 (br d, 13.4 Hz, 2H, NCHH′Ar cis to CHO), 4.08 (br d, 13.4 Hz, 2H, NCHH′Ar cis to CHO), 7.02 (sl br s, 3H, ArH), 7.09 (sl br s, 2H, ArH), 7.24 (br s, 1H, ArH), 7.49 (d, 1.9 Hz, 1H, cresol ArH), 8.01 (d, 1.9 Hz, 1H, cresol ArH), 9.15 (s, 1H, bound CHO), 10.82 (s, 1H, free CHO). ^{13}C{^{1}H} NMR (CD_2Cl_2, 273 K): δ 20.27, 29.76, 30.08, 31.86, 34.58, 34.65, 35.01, 35.54, 61.56, 123.71, 123.79, 124.44, 124.98, 125.61, 126.44, 126.54, 128.70, 135.05, 135.62, 139.13, 141.57, 142.98, 143.17, 158.32, 160.83, 167.33, 189.92, 194.05. IR: 1691 (m), 1638 (s), 1552 (m), 969 (w), 840 (m). EI-MS: 879 (M$^+$).

1,5-Dioxyanthraquinonebis{[nitrilotris(3,5-di-*tert*-butyl-2-cresolato)]titanium(IV)}, (LTi)$_2$(anruf). 200 mg of LTi(O^{t}Bu) (0.253 mmol) and 32 mg of anthrarufin (0.133 mmol, 0.53 equiv) were dissolved in 20 mL of benzene. The solution was refluxed for 2 h, changing color from yellow to orange to red in a few minutes. The volatiles were removed on a rotary evaporator to leave behind a red solid. The solid was redissolved in hexane (10 mL), and 50 mL of acetone was added to the solution. The solution was placed in a −20 °C freezer for 2 days after which small red crystals had precipitated. The solid was recrystallized by dissolving it in a minimum of benzene and layering with 20 mL of CH_3CN. After 24 h, the red crystals of (LTi)$_2$(anruf) were filtered on a glass frit, washed with CH_3CN (3 × 5 mL), and air-dried. Yield: 102 mg (48%). ^{1}H NMR (CD_2Cl_2, 273 K; the molecule has $\sim C_{2h}$ symmetry on the NMR time scale at this temperature): δ 0.86 (s, 36H, ^{t}Bu), 1.25 (s, 54H, ^{t}Bu), 1.56 (s, 18H, *t*-Bu), 3.70 (br s, 4H, NCH_2Ar trans to quinone), 3.76 (br s, 4H, NCHH′Ar cis to quinone), 4.03 (br s, 4H, NCHH′Ar cis to quinone), 6.31 (dd, 7.4, 1.3 Hz, 2H, anruf 4,8-H), 6.98 (sl br s, 4H, ArH), 7.03 (sl br s, 6H, ArH), 7.12 (dd, 8.6, 1.3 Hz, 2H, anruf 2,7-H), 7.26 (br s, 2H, ArH), 7.32 (dd, 8.6, 7.4 Hz, 2H, anruf 3,6-H). ^{13}C{^{1}H} NMR (C_6D_6, 323 K): δ 30.56, 32.40, 34.85, 35.60, 61.94, 120.43, 120.98, 124.08, 124.54, 125 (very broad), 129.19, 134.49, 136.09 (broad), 137.96, 141.99 (broad), 159.9 (very broad), 168.56, 184.16. IR: 1611 (s), 1585 (s), 1532 (w), 1469 (m), 1330 (w), 1094 (w), 1060 (w). FAB-MS: 1672 (M + H). Anal. Calcd for $C_{104}H_{138}N_2O_{10}Ti_2$: C, 74.71; H, 8.32; N, 1.68. Found: C, 75.09; H, 8.45; N, 1.62.

Di-μ-(dibenzylphosphato)bis[nitrilotris(3,5-di-*tert*-butyl-2-cresolato)]dititanium(IV), {LTi[O$_2$P(OCH$_2$Ph)$_2$]}$_2$. To a solution of 200 mg of LTi(O^{t}Bu) (0.253 mmol) dissolved in 20 mL of dichloromethane was added dibenzyl phosphate (75 mg, 0.270 mmol, 1.07 equiv), causing an immediate color change from yellow to red. The solution was stirred for 1 h at room temperature,

and the volatiles were removed on a rotary evaporator to give a reddish-orange solid, which was a mixture of $\{LTi[O_2P(OCH_2Ph)_2]\}_2$ and unreacted LTiO^{t}Bu as determined by NMR. The solid was dissolved in a minimum of hexane and loaded onto a silica gel column. The column was eluted with hexane, and the fast-moving reddish-orange band was collected. The compound was then recrystallized by dissolving it in a minimum of dichloromethane and layering with CH_3CN (20 mL). Red crystals, which were suitable for X-ray analysis, formed within 24 h. The crystals were filtered, washed with CH_3CN (3 × 5 mL), and dried on a glass frit to yield 91 mg (36%) of $\{LTi[O_2P(OCH_2Ph)_2]\}_2$. ^{1}H NMR ($C_6D_6$): δ 1.19 (s, 18H, ^{t}Bu), 1.41 (s, 36H, ^{t}Bu), 1.45 (s, 36H, ^{t}Bu), 1.50 (s, 18H, ^{t}Bu), 3.10 (d, 13.5 Hz, 4H, NC*H*H′Ar cis to phosphate), 3.15 (s, 4H, NCH_2Ar trans to phosphate), 4.91 (d, 13.5 Hz, 4H, NCH*H*′Ar cis to phosphate), 5.20, 5.27 (dd, 12.3, 6.5 Hz, 4H ea., POC*HH*′Ph), 6.22 (d, 2.5 Hz, 2H, Ar*H*), 6.83−7.13 (m, 26 H, Ar*H* (6H), POCH$_2$*Ph* (20 H)), 7.33 (d, 2.5 Hz, 4H, Ar*H*). ^{13}C{^{1}H} NMR (CD_2Cl_2): δ 30.94, 31.24, 31.84, 32.12, 34.20, 34.62, 35.22, 35.26, 60.47, 66.35, 68.82 (d, 5.5 Hz), 123.14, 123.65, 124.01, 126.08, 126.38, 127.36, 128.06, 128.66, 131.26, 134.52, 137.43, 137.55, 141.01, 141.23, 160.25, 161.80. ^{31}P NMR (CD_2Cl_2): δ −11.93 (quintet, J_{PH} = 6.5 Hz). IR: 1456 (m), 1391 (w), 1200 (s), 1053 (m), 1026 (m), 843 (m), 695 (w). FAB-MS: 1986 (M − H), 994 (LTi(O_2P[$OCH_2Ph]_2$) + H). The analytical sample retained half a mole of dichloromethane. Anal. Calcd for $C_{118.5}H_{161}ClN_2O_{14}P_2Ti_2$: C, 70.09; H, 7.99; N, 1.38. Found: C, 69.76; H, 7.76; N, 1.47.

Variable-Temperature NMR Studies. Samples were prepared by dissolving 10−20 mg of the desired compound in 0.5 mL of CD_2Cl_2 in a drybox in a 5-mm NMR tube with a screw cap. Spectra were acquired on a Varian VXR-500 NMR spectrometer at temperatures between −100 and +40 °C. Rate constants for the dynamic processes were determined by full line-shape analysis using the program gNMR.[14] The rate of the twisting (racemization) process was generally analyzed using the exchange of the two most upfield *tert*-butyl resonances (ortho to the phenoxides on the mutually trans arms of the tripod ligand). For LTi(dtm), the exchange of the resonances due to the *tert*-butyl groups para to the phenoxides was also simulated, and the rate constants were averaged. For LTi(trop), arm interchange was rapid at all temperatures studied, making this procedure impossible, so for this compound the racemization rate constant was obtained by simulating the exchange of axial and equatorial hydrogens on the CH_2 groups. The rate of arm interchange was generally measured using the exchange of the resonances of the *tert*-butyl groups ortho to the phenoxides on the unique arm (trans to the bidentate chelate) with those on the two other arms. (The chemical shift dispersion of the para *tert*-butyl groups was invariably too small for these resonances to be useful.) For LTi(dtm), the arm interchange rate was determined to be the same, within experimental error, as the rate of interchange of the tolyl methyl groups at all temperatures at which they were measured, and both values were averaged in the determination of the activation parameters for the reaction. For LTi(acac), it was not possible to measure the arm interchange rate by analysis of the *tert*-butyl region, so the value measured by interchange of the acac methyl groups was used. In LTi(hq), arm interchange and twisting occur at comparable rates, and the *tert*-butyl region was successfully simulated with simultaneous determination of both rate constants. The rate of exchange of the bound and free aldehydes in LTi(dfc) was measured by simulating the exchange of the two formyl C*H*O and the two diformylcresolate aromatic resonances. It was assumed that this process also contributes to the rate of arm interchange, and so this rate (multiplied by a statistical factor of $^4/_3$) was subtracted from the measured overall rate of arm interchange to give the rate constant for direct (nondissociative) arm interchange.

X-ray Crystallography of LTi(trop), LTi(acac), LTi(hq)·CH_3CN·0.5C_6H_6, and LTi(dfc)·CH_2Cl_2. Crystals of LTi(trop), LTi(acac), and LTi(hq) were grown through slow diffusion of CH_3CN into benzene solutions of the complexes; crystals of LTi(dfc) were grown by diffusion of CH_3CN into CH_2Cl_2. Suitable crystals were placed in inert oil and transferred to the tip of a glass fiber in the cold N_2 stream of a Bruker Apex CCD diffractometer (T = 100 K). Data were reduced, correcting for absorption and decay, using the program SADABS. The space groups of the monoclinic crystals were determined by their systematic absences; the hydroxyquinolinate crystal was triclinic and was solved and refined successfully in the space group $P\bar{1}$. The titanium atoms in LTi(trop) and LTi(dfc)·CH_2Cl_2 were found on Patterson maps; LTi(acac) and LTi(hq)·CH_3CN·0.5C_6H_6 were solved using direct methods. Remaining nonhydrogen atoms were found on difference Fourier maps. All heavy atoms were refined anisotropically, and hydrogens were placed in calculated positions. All of the calculations used SHELXTL (Bruker Analytical X-ray Systems), with scattering factors and anomalous dispersion terms taken from the literature.[15] Further details about the individual structures may be found in Table 1.

X-ray Crystallography of $\{LTi[O_2P(OCH_2Ph)_2]\}_2$·4$CH_2Cl_2$. Crystals of $\{LTi[O_2P(OCH_2Ph)_2]\}_2$ were grown by diffusion of CH_3CN into CH_2Cl_2. Data acquisition and reduction were as described above. The systematic absences exhibited by the monoclinic crystal were consistent with the space group $C2/c$, except that a significant number of the reflections expected to be absent due to the c glide were observed with $I > 3\sigma(I)$, although these reflections were generally weak (avg $I/\sigma(I)$ = 3.3). The structure was successfully solved and refined in $C2/c$, with the dimeric titanium complex on the crystallographic inversion center. Solution of the structure ignoring the presence of the glide plane (space group $C2$) was possible, but refinement was poorly behaved, with many atoms unable to be refined anisotropically. There was substantial disorder in the structure. One of the *tert*-butyl groups (methyls bonded to C120) was disordered over two different orientations (major orientation = 74.7(7)%). One of the benzyloxy groups was also found in two different orientations, with the major orientation refining to 58.3(3)% occupancy. The phenyl groups in this disordered benzyloxy group were modeled as rigid hexagons. One dichloromethane molecule was found in two orientations, one of which was unreasonably close to one of the benzyloxy conformers, so the occupancies of the two solvent orientations were fixed to the complementary benzyloxy occupancies. Thermal parameters for one of the remaining dichloromethanes indicated partial occupancy, and it was arbitrarily refined at half occupancy. All non-hydrogen atoms were refined anisotropically, and hydrogen atoms were placed in calculated positions.

Results

Synthesis and Structure of Bidentate Chelates of Nitrilotris(3,5-di-*tert*-butyl-2-cresolato)titanium(IV). A five-coordinate titanium complex of triply deprotonated tris(2-hydroxy-3,5-di-*tert*-butylbenzyl)amine), LTi(O^{i}Pr), was reported by Kol and co-workers.[6] The analogous light yellow

(14) Budzelaar, P. H. M. *gNMR* v.3.6.5; Cherwell Scientific Publishing: Oxford, 1996.

(15) *International Tables of Crystallography*; Kluwer Academic Publishers: Dordrecht, The Netherlands, 1992; Vol. C.

Table 1. X-ray Crystallographic Details for LTi(trop), LTi(acac), LTi(hq)·CH_3CN·$0.5C_6H_6$, LTi(dfc)·CH_2Cl_2, and $\{LTi[O_2P(OCH_2Ph)_2]\}_2$·$4CH_2Cl_2$

	LTi(trop)	LTi(acac)	LTi(hq)·CH_3CN·$0.5C_6H_6$	LTi(dfc)·CH_2Cl_2	$\{LTi[O_2P(OCH_2Ph)_2]\}_2$·$4CH_2Cl_2$
empirical formula	$C_{52}H_{71}NO_5Ti$	$C_{50}H_{73}NO_5Ti$	$C_{59}H_{78}N_3O_4Ti$	$C_{55}H_{75}Cl_2NO_6Ti$	$C_{122}H_{168}Cl_8N_2O_{14}P_2Ti_2$
fw	838.00	815.99	941.14	964.96	2327.92
temp (K)	100(2)	100(2)	100(2)	100(2)	100(2)
λ, Å	0.71073 (Mo Kα)	0.71073 (Mo Kα)	0.71073 (Mo Kα)	0.71073 (Mo Kα)	0.71073 (Mo Kα)
space group	$P2_1/c$	$P2_1/c$	$P\bar{1}$	$P2_1/n$	$C2/c$
total data collected	51 287	51 108	19 331	47 640	64 921
no. of indep reflns	12 059	12 054	9283	13 009	15 322
R_{int}	0.0317	0.0279	0.0468	0.0548	0.0503
obsd reflns [$I > 2\sigma(I)$]	10 329	10 401	6657	9711	12 120
a (Å)	23.5527(12)	14.4659(7)	12.6377(8)	20.6770(9)	27.0249(18)
b (Å)	11.1270(5)	11.9192(6)	14.5709(9)	11.7837(5)	13.5399(9)
c (Å)	19.8941(10)	28.9215(15)	16.8667(10)	22.4263(10)	34.491(2)
α (deg)	90	90	81.1100(10)	90	90
β (deg)	111.2940(10)	103.0750(10)	69.2120(10)	106.3570(10)	101.6600(10)
γ (deg)	90	90	65.4030(10)	90	90
V (Å^3)	4857.7(4)	4857.4(4)	2640.1(3)	5243.0(4)	12 360.2(14)
Z	4	4	2	4	4
calcd ρ (g/cm^3)	1.146	1.116	1.184	1.222	1.251
cryst size (mm)	0.48 × 0.18 × 0.09	0.43 × 0.28 × 0.18	0.30 × 0.15 × 0.15	0.27 × 0.10 × 0.08	0.40 × 0.30 × 0.30
μ (mm^{-1})	0.221	0.219	0.210	0.314	0.387
no. refined params	532	518	605	586	725
R indices [$I > 2\sigma(I)$][a]	R1 = 0.0426 wR2 = 0.1096	R1 = 0.0429 wR2 = 0.1167	R1 = 0.0475 wR2 = 0.1054	R1 = 0.0817 wR2 = 0.2183	R1 = 0.0966 wR2 = 0.2617
R indices (all data)[a]	R1 = 0.0507 wR2 = 0.1155	R1 = 0.0500 wR2 = 0.1234	R1 = 0.0754 wR2 = 0.1189	R1 = 0.1070 wR2 = 0.2438	R1 = 0.1145 wR2 = 0.2758
GOF	1.018	1.019	1.005	1.012	1.076

[a] $R1 = \sum||F_o| - |F_c||/\sum|F_o|$; $wR2 = (\sum[w(F_o^2 - F_c^2)^2]/\sum w(F_o^2)^2)^{1/2}$.

titanium(IV) *tert*-butoxide LTi(O^{t}Bu)[11] reacts rapidly with the symmetrical, bidentate enolic ligands tropolonate (trop), acetylacetonate (acac), and di-*p*-toluoylmethanide (dtm) in their protonated forms. An equivalent of *tert*-butyl alcohol is liberated and chelated, six-coordinate complexes of the LTi(IV) moiety are produced in good yield (eq 1).

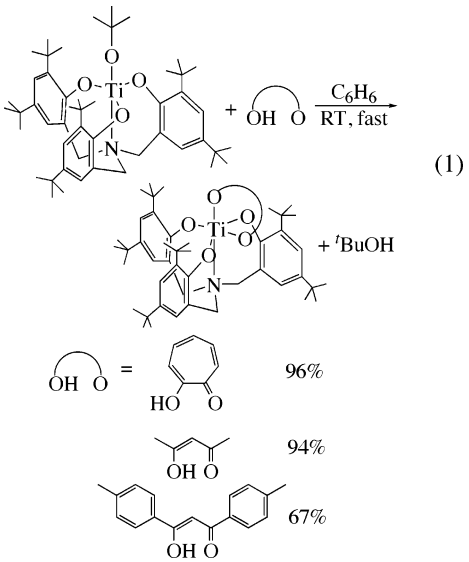

(1)

Phenols with pendant donors, such as 8-hydroxyquinoline (Hhq), salicylaldehyde (Hsal), and 2,6-diformyl-*p*-cresol (Hdfc), react similarly, but more slowly, with reactions going to completion within several hours in refluxing benzene or dichloromethane (eq 2). Anthrarufin (1,5-dihydroxyanthraquinone, H_2anruf) reacts analogously with 2 equiv of LTi(O^{t}Bu) to give the complex $(LTi)_2$(anruf) where an LTi moiety is bonded to each phenoxy group. A 1:1 complex, LTi(Hanruf), can be observed by NMR in reactions using a 1:1 mixture of LTi(O^{t}Bu) and H_2anruf, but it is always mixed with starting material and $(LTi)_2$(anruf) and was not isolated in pure form.

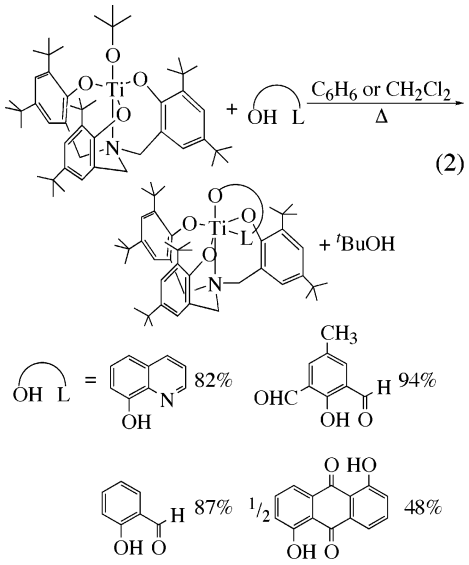

(2)

The structures of four of these complexes, LTi(trop) (Figure 1), LTi(acac) (Figure 2), LTi(hq) (Figure 3), and LTi(dfc) (Figure 4), have been determined by X-ray crystallography (Tables 1 and 2). The structures of all four compounds are quite similar and have several noteworthy features. The complexes are roughly octahedral with the bidentate ligand occupying both an axial position (trans to the central amine nitrogen of the nitrilotricresolate ligand)

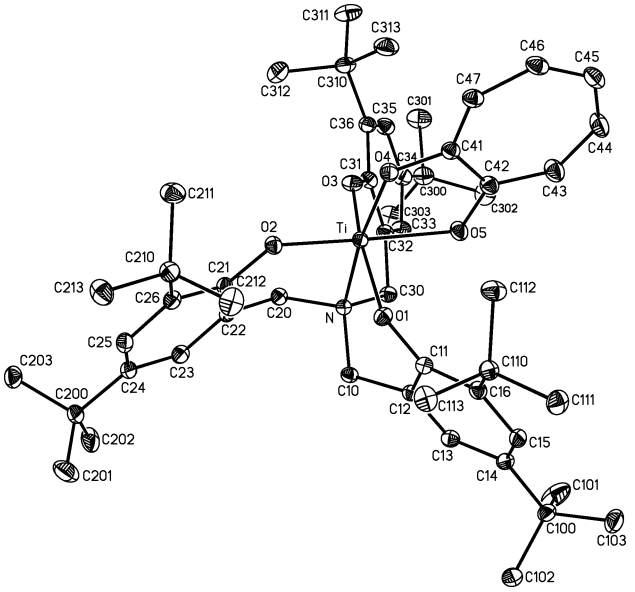

Figure 1. SHELXTL plot (40% thermal ellipsoids) of LTi(trop).

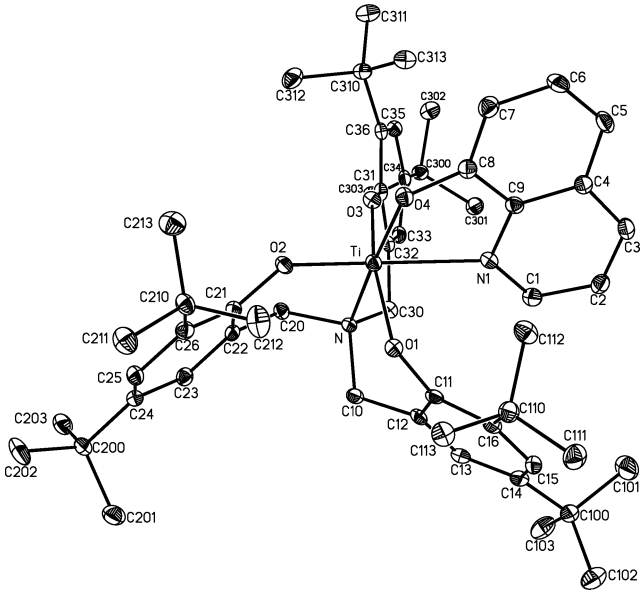

Figure 3. SHELXTL plot (40% thermal ellipsoids) of LTi(hq).

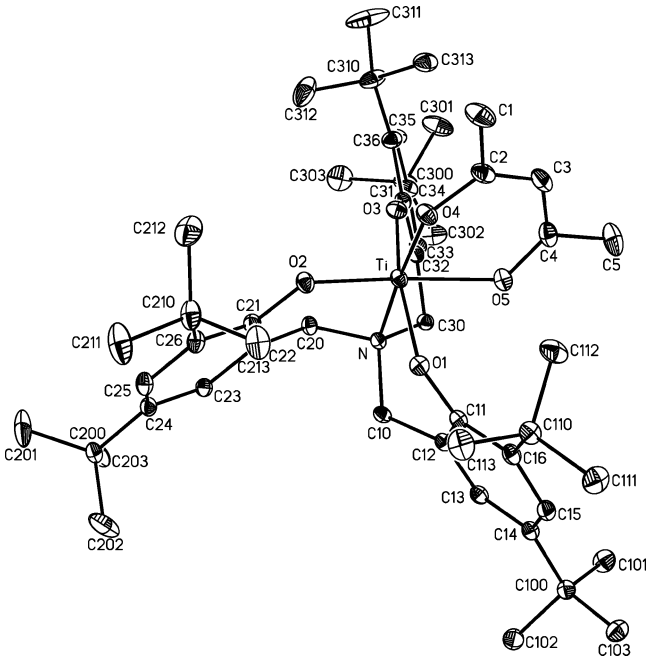

Figure 2. SHELXTL plot (40% thermal ellipsoids) of LTi(acac).

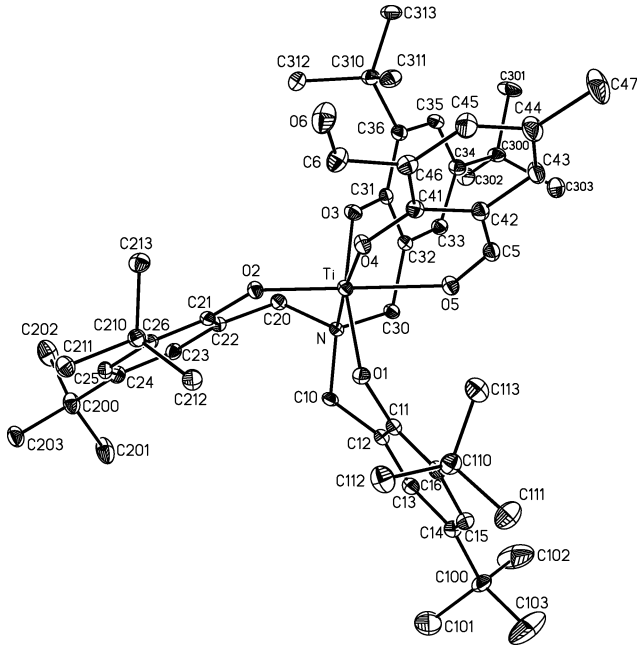

Figure 4. SHELXTL plot (40% thermal ellipsoids) of LTi(dfc).

and an equatorial position (trans to one of the tripodal phenoxide ligands). While these are the first examples of octahedral titanium complexes with the nitrilotris(cresolate) ligand,[6−7,11] the ability of such ligands to support octahedral geometries is well-established in tantalum complexes of the related $N(CH_2C_6H_2Me_2O)_3$ ligand.[8] That the tripodal ligand experiences some strain in achieving an octahedral geometry is indicated by the relatively acute "trans" angle O1−Ti−O3 (159° avg in the four complexes), similar to the angles seen in the tantalum complexes.[8] However, in contrast to the tantalum complexes, the tripodal ligand retains the pseudo-C_3 propeller-like conformation it adopts in the trigonal bipyramidal LTiX complexes in these octahedral complexes. The complexes thus have C_1 symmetry, with the phenyl group of one of the aryloxides cis to the bidentate chelate pointed at it and the other pointed away. This generates a significant steric clash between the bidentate chelate and the aryloxide, which is partially relieved by tilting of the plane of the bidentate ligand out of the Ti−N−O2 plane, away from the intruding aryloxide (by 6.6°, 18.5°, 22.5°, and 17.1° in the four structures).

The inequivalence of the two groups bound trans to the bidentate chelate (neutral nitrogen N and phenoxide oxygen O2) generates asymmetry in the binding of the nominally symmetric tropolonate and acetylacetonate ligands. As expected, the greater trans influence of the phenoxide significantly elongates the equatorial Ti−O5 bond relative to the axial Ti−O4 bond (by 0.1330(14) Å in the tropolonate and 0.1355(14) Å in the acetylacetonate). The asymmetry in Ti−O distances is reflected in perceptible bond alternation

Table 2. Selected Bond Distances (Å) and Angles (deg) for LTi(trop), LTi(acac), LTi(hq)·CH_3CN·$0.5C_6H_6$, LTi(dfc)·CH_2Cl_2, and $\{LTi[O_2P(OCH_2Ph)_2]\}_2$·$4CH_2Cl_2$

	LTi(trop)	LTi(acac)	LTi(hq)·CH_3CN·$0.5C_6H_6$	LTi(dfc)·CH_2Cl_2	$\{LTi[O_2P(OBn)_2]\}_2$·$4CH_2Cl_2$
Ti−O1	1.8974(10)	1.8811(10)	1.911(2)	1.867(2)	1.877(2)
Ti−O2	1.8259(9)	1.8382(10)	1.829(2)	1.828(2)	1.870(2)
Ti−O3	1.8746(10)	1.8714(10)	1.864(2)	1.882(2)	1.875(2)
Ti−N	2.2386(11)	2.2518(11)	2.272(2)	2.245(3)	2.249(3)
Ti−O4	1.9643(9)	1.9452(10)	1.913(2)	1.928(2)	1.964(3)
Ti−O5	2.0973(10)	2.0807(10)		2.161(2)	2.055(3)
Ti−N1			2.346(2)		
O1−Ti−O2	94.39(4)	94.70(4)	94.38(7)	98.31(10)	88.63(10)
O1−Ti−O3	161.03(4)	160.35(4)	158.28(7)	157.50(10)	166.52(11)
O2−Ti−O3	96.42(4)	97.95(4)	99.82(7)	97.30(10)	93.69(11)
N−Ti−O1	84.21(4)	84.53(4)	84.31(7)	84.22(9)	84.99(10)
N−Ti−O2	87.93(4)	87.33(4)	87.60(7)	86.82(10)	86.89(11)
N−Ti−O3	80.66(4)	81.12(4)	79.99(7)	80.57(9)	81.88(11)
N−Ti−O4	170.82(4)	173.12(4)	170.07(7)	173.33(10)	175.90(15)
N−Ti−O5	94.70(4)	89.71(4)		89.76(9)	87.90(15)
N−Ti−N1			98.19(7)		
O1−Ti−O4	98.10(4)	99.03(4)	102.44(7)	98.47(10)	94.73(12)
O2−Ti−O4	100.71(4)	98.19(4)	99.01(7)	98.78(10)	97.19(15)
O3−Ti−O4	95.15(4)	93.99(4)	91.53(7)	95.04(10)	98.15(12)
O1−Ti−O5	85.68(4)	83.42(4)		82.91(9)	87.94(11)
O2−Ti−O5	177.37(4)	176.64(4)		176.22(9)	174.00(14)
O3−Ti−O5	84.22(4)	83.15(4)		80.55(9)	88.53(12)
O1−Ti−N1			82.16(7)		
O2−Ti−N1			172.89(7)		
O3−Ti−N1			85.32(7)		
O4−Ti−O5	76.68(4)	84.88(4)		84.54(9)	88.00(18)
O4−Ti−N1			75.81(7)		
Ti−O4−P					165.1(2)
Ti−O5−P0A					165.1(3)
O4−P−O5A					115.8(3)

in the bidentate chelate, which is larger in the acetylacetonate (0.032 Å avg) than in the tropolonate (0.016 Å avg). The unsymmetrical chelates 8-hydroxyquinolinate and diformylcresolate reflect the trans influence of the tripod in their observed regioisomers, with the phenoxide group apical and the neutral donor equatorial. In solution, only one regioisomer of all of the unsymmetrical chelates is observed, and by comparison to these two structures it is presumed to be the one with the phenoxide donor apical.

Variable-Temperature NMR Spectroscopy of Bidentate Chelates of Nitrilotris(3,5-di-*tert*-butyl-2-cresolato)titanium(IV). ^{1}H NMR spectra of the bidentate chelate complexes are consistent with the retention in solution of the chiral, C_1-symmetric structures exhibited in the solid state, as illustrated for LTi(dtm) (Figure 5) and LTi(dfc) (Figure 6). At low temperatures, the spectra generally exhibit six 2 Hz doublets due to the aryl protons of the tripod, six doublets with coupling constants of 13−15 Hz for the diastereotopic methylene protons, and six singlets for the *tert*-butyl resonances, as well as the resonances due to the bidentate chelate. As the temperature is raised, two fluxional processes are generally observed. At temperatures between about −90 and −60 °C, there is a process that interconverts two of the aryl environments of the tripod, but leaves the third set of aryl environments unaffected. (This process also interconverts the axial and equatorial hydrogens of the NCH_2 groups, although the line shape in the methylene region is usually complex and was not analyzed in detail.) This process corresponds to a twisting of the tripodal ligand's benzyl groups, which inverts the helical sense of the tripod but does not affect the first coordination sphere of titanium. This motion establishes an effective time-averaged mirror plane containing the bidentate ligand, the central tertiary amine, and the tripod phenoxide trans to the bidentate chelate; it renders the two tripod phenoxides trans to each other equivalent.

A second fluxional process, usually seen at higher temperatures (above ∼0 °C for both LTi[dtm] and LTi[dfc]), renders all of the phenoxide groups of the tripod equivalent. At the same time, in LTi(dtm), the resonances for the two tolyl groups of the ditoluoylmethane ligand also broaden and coalesce as the two ends of the bidentate ligand exchange. The other complexes of symmetrical bidentate ligands show the same qualitative behavior. Although the rate of arm exchange in LTi(acac) could not be measured quantitatively, it occurs in the same temperature range as acac methyl group exchange, and both arm exchange and ligand end exchange are too fast to measure in LTi(trop). (This kind of exchange is of course impossible for the unsymmetrical chelates such as hydroxyquinoline or salicylaldehyde.)

Quantitatively, the rates of exchange in LTi(dtm) measured from the tolyl methyl groups and from the *tert*-butyl groups are identical within experimental error (Figure 7). This is consistent with a motion that slides the bidentate ligand from one cleft in the tripod to another with the bidentate ligand moving like a windshield wiper blade, such that each time the ligand switches clefts in the tripod it also interchanges ligand ends (Scheme 1a). One could also imagine a motion where the bidentate ligand ends and its position in the tripod clefts were interchanged statistically, for example by moving the bidentate ligand so that its two-fold axis coincides with the tripod's three-fold axis, followed by mutual rotation of

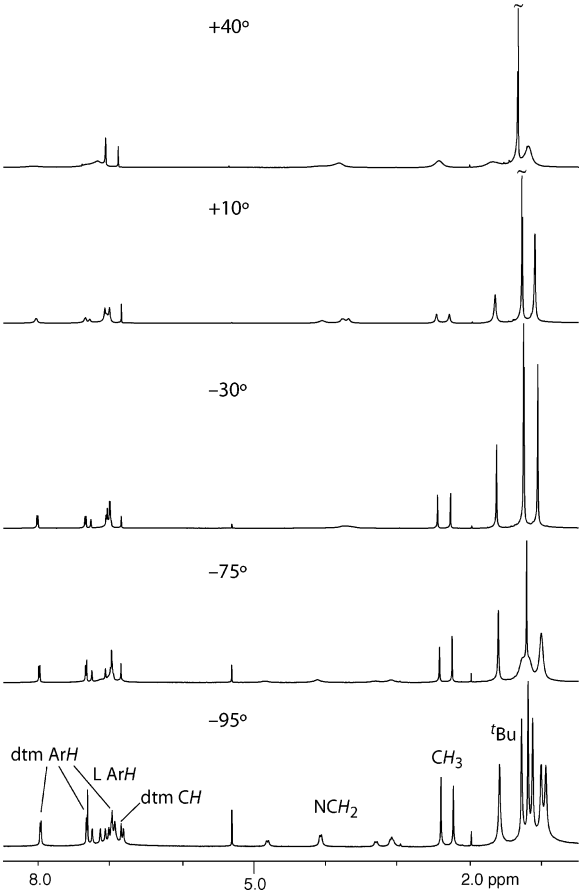

Figure 5. Variable-temperature ^{1}H NMR spectra (CD_2Cl_2, 500 MHz) of LTi(dtm). Temperatures are given in °C.

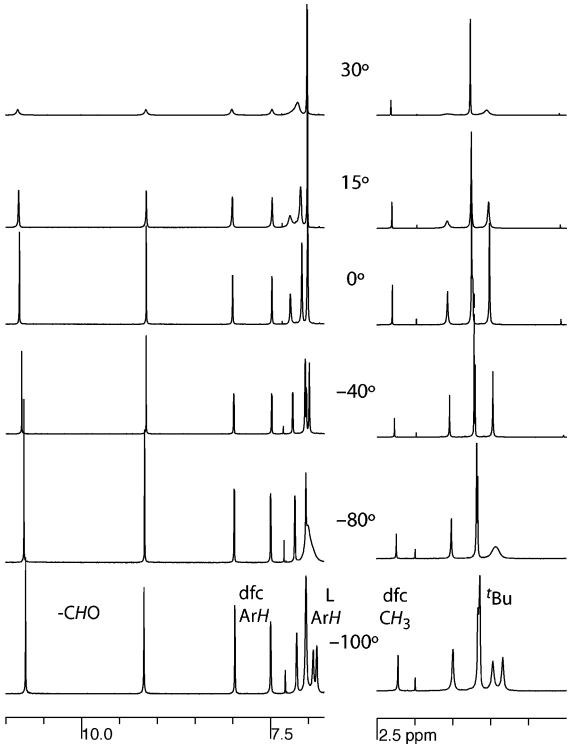

Figure 6. Variable-temperature ^{1}H NMR spectra (CD_2Cl_2, 500 MHz) of LTi(dfc), with temperatures in °C. The region from 2.5 to 7.5 ppm (which includes the CH_2 resonances) is omitted. The vertical scale of the upfield (*tert*-butyl and methyl) region is reduced relative to the downfield region, but the horizontal scale is constant in the plot.

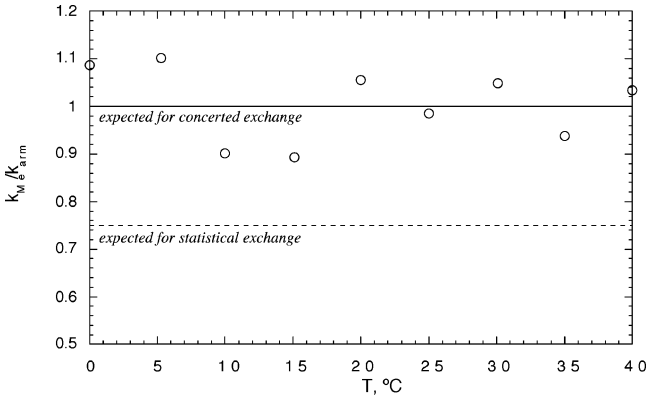

Figure 7. Ratio of rate constants measured in CD_2Cl_2 for tolyl methyl group exchange (k_{Me}) and for tripod arm *tert*-butyl group exchange (k_{arm}) in LTi(dtm) as a function of temperature. The solid line indicates the ratio predicted by synchronous rearrangement (Scheme 1a), and the dashed line indicates that predicted by statistical rearrangement (Scheme 1b).

the two groups around their common axis before the bidentate ligand collapses to its equilibrium position (Scheme 1b). However, because each such "sit-and-spin" motion would result in a change in tripod orientation two-thirds of the time but a change in bidentate ligand only one-half of the time, such a motion would predict a k_{Me}/k_{arm} ratio of 3/4, which is clearly excluded by the data.

The activation parameters for ligand flexing and for tripod arm exchange for the seven complexes, derived from Eyring plots of the rate data (Figures S2 and S3), are compiled in Table 3. While the pattern described above is typical, there are a few noteworthy deviations. Most significantly, the tropolonate ligand in LTi(trop) is symmetrical by NMR, and all of the aryl groups of the tripod are equivalent, even at −100 °C, suggesting that the arm interchange process is extremely fast. However, the methylene protons decoalesce at low temperatures into a pair of mutually coupled doublets (Figure S1), allowing the rate of ligand racemization to be measured. The fact that arm interchange is much faster than ligand twisting in this complex, but comparable in rate in LTi(hq), and much slower in the other complexes, indicates that the two mechanisms operate independently of one another. In the anthrarufin complex $(LTi)_2$(anruf), the ligand twisting motion is complicated by the presence of two diastereomers (a *meso* and *dl* pair, depending on the relative configuration of the two tripodal ligands), which can be discerned at low temperature by the presence of two distinct peaks for the 2,6-H resonances of the anthrarufin (δ 6.04 and 5.83, in a 2:1 ratio, at −100 °C). Qualitatively, the twisting motion leads to spectral changes, ultimately averaging the two diastereomers and the mutually trans phenoxides within each diastereomer, between about −90 and −60 °C, but the rates were not measured quantitatively due to the complexity of the spectra. The rate of the twisting motion was not determined for LTi(acac) due to poor chemical shift dispersion of the *tert*-butyl resonances.

Finally, the latent symmetry of the 2,6-diformyl-*p*-cresolate ligand allows one to address the possibility of dissociation of the neutral aldehyde donor, which would allow exchange

Scheme 1. Possible Intramolecular Mechanisms for Tripod Arm Exchange in Six-Coordinate Complexes: (a) Concerted, or "Ballistic", Mechanism; (b) Statistical, or "Sit-and-Spin", Mechanism, Characterized by a Long-Lived Nonoctahedral Intermediate

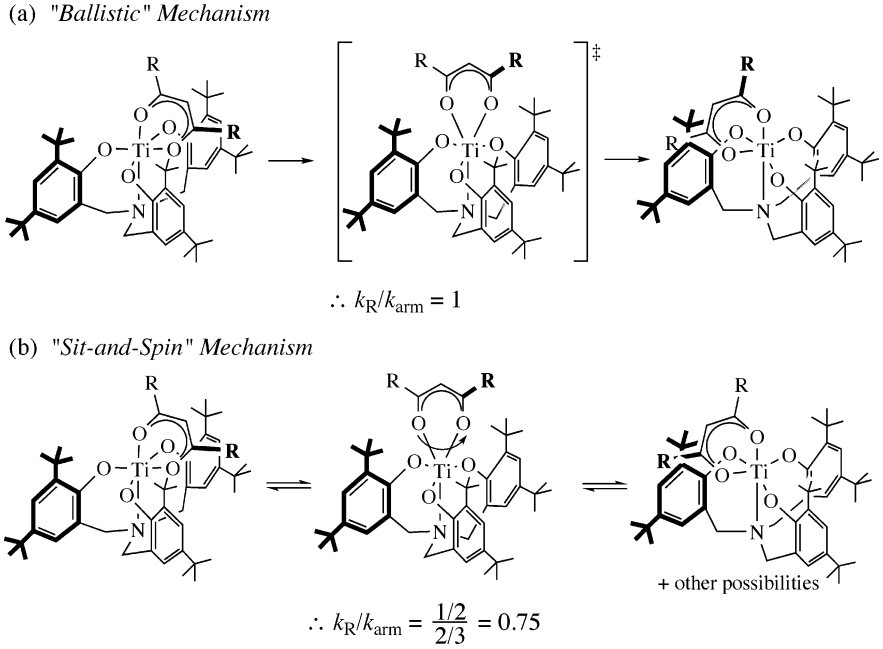

Table 3. Activation Parameters for Fluxional Processes in LTiX Complexes (Except As Noted, All Data Were Obtained in CD_2Cl_2, and All $\Delta G^{\ddagger}$ Values Are Reported at 300 K; na = Not Applicable)

apical ligand	racemization	arm interchange	dissociation
O^{i}Pr[a]	$\Delta G^{\ddagger}$ = 17.8 kcal/mol[b]	na	na
tropolonate	$\Delta H^{\ddagger}$ = 10.7(6) kcal/mol $\Delta S^{\ddagger}$ = +7(3) eu $\Delta G^{\ddagger}$ = 8.6(11) kcal/mol	too fast to measure at −100 °C	na
8-hydroxyquinolinate	$\Delta H^{\ddagger}$ = 8.46(17) kcal/mol $\Delta S^{\ddagger}$ = −10.2(8) eu $\Delta G^{\ddagger}$ = 11.5(3) kcal/mol	$\Delta H^{\ddagger}$ = 11.58(7) kcal/mol $\Delta S^{\ddagger}$ = +4.4(3) eu $\Delta G^{\ddagger}$ = 10.26(11) kcal/mol	na
acetylacetonate	not measured	$\Delta H^{\ddagger}$ = 7.65(20) kcal/mol $\Delta S^{\ddagger}$ = −11.9(9) eu $\Delta G^{\ddagger}$ = 11.2(3) kcal/mol	na
salicylaldehyde	$\Delta H^{\ddagger}$ = 7.14(18) kcal/mol $\Delta S^{\ddagger}$ = −11.3(9) eu $\Delta G^{\ddagger}$ = 10.5(3) kcal/mol	$\Delta H^{\ddagger}$ = 12.46(10) kcal/mol $\Delta S^{\ddagger}$ = +2.7(4) eu $\Delta G^{\ddagger}$ = 11.66(16) kcal/mol	na
anthrarufin	not measured	$\Delta H^{\ddagger}$ = 9.57(13) kcal/mol $\Delta S^{\ddagger}$ = −15.1(5) eu $\Delta G^{\ddagger}$ = 14.10(20) kcal/mol	na
diformylcresolate	$\Delta H^{\ddagger}$ = 7.29(23) kcal/mol $\Delta S^{\ddagger}$ = −9.4(12) eu $\Delta G^{\ddagger}$ = 10.1(4) kcal/mol	$\Delta H^{\ddagger}$ = 13.6(4) kcal/mol[c,d] $\Delta S^{\ddagger}$ = −2.4(12) eu[c,d] $\Delta G^{\ddagger}$ = 14.3(5) kcal/mol[c,d]	$\Delta H^{\ddagger}$ = 17.0(6) kcal/mol[c] $\Delta S^{\ddagger}$ = +4.8(18) eu[c] $\Delta G^{\ddagger}$ = 15.6(8) kcal/mol[c]
di-*p*-toluoylmethane	$\Delta H^{\ddagger}$ = 7.1(3) kcal/mol $\Delta S^{\ddagger}$ = −12.4(16) eu $\Delta G^{\ddagger}$ = 10.9(6) kcal/mol	$\Delta H^{\ddagger}$ = 11.52(12) kcal/mol $\Delta S^{\ddagger}$ = −10.3(4) eu $\Delta G^{\ddagger}$ = 14.61(17) kcal/mol	na

[a] Reference 6. [b] 386 K, $C_6D_5NO_2$. [c] $CDCl_3$. [d] These values are for the overall rate of arm interchange, which includes a contribution from the dissociative mechanism. If this contribution is subtracted, the activation parameters for the nondissociative interchange are: $\Delta H^{\ddagger}$ = 12.6(3) kcal/mol, $\Delta S^{\ddagger}$ = −6.2(11) eu, $\Delta G^{\ddagger}$ = 14.5(4) kcal/mol.

between the bound and free aldehydes (as well as the two aryl protons on the cresolate). At temperatures below about 10 °C, this exchange does not take place at a sufficiently fast rate to be observable by NMR, but exchange does begin to set in at higher temperatures (Figure 6). This exchange takes place at similar temperatures to the arm interchange process, but close examination of the spectra clearly shows that the aldehyde dissociation is noticeably *slower* than arm interchange. This is most evident in the 0 and 15 °C spectra in Figure 6, where the tripod aryl (and *tert*-butyl) resonances have already begun to show significant broadening, while the cresolate aryl and aldehyde resonances remain rather sharp. The activation parameters of the two processes are also quite different, with the dissociative pathway exhibiting

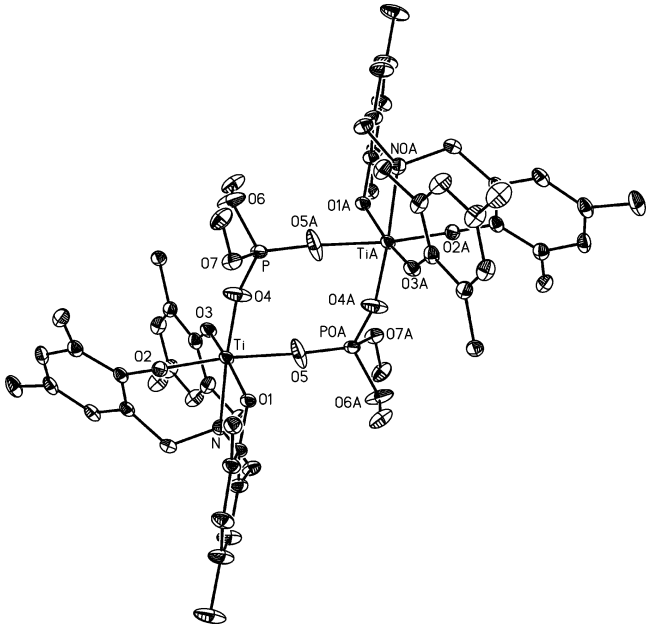

Figure 8. SHELXTL plot (40% thermal ellipsoids) of the titanium complex in $\{LTi(\mu\text{-}O_2P[OCH_2Ph]_2)\}_2 \cdot 4CH_2Cl_2$. Phenyl groups of the dibenzyl phosphates and *tert*-butyl methyl groups have been omitted for clarity.

a higher enthalpy of activation and more positive entropy of activation, as expected (Table 3, Figure S4). Dissociation of the neutral aldehyde presumably leads to a five-coordinate complex in which the arms of the tripod are equivalent. However, even when this contribution to the overall rate of tripod arm interchange is subtracted, the rate of nondissociative arm interchange exceeds the rate of aldehyde dissociation by a factor of 3−10 in the temperature range where both can be measured. Thus, aldehyde dissociation is only a minor contributor to arm interchange in LTi(dfc).

Preparation, Structure, and Dynamics of the Dimeric Dibenzyl Phosphate Complex $\{LTi[O_2P(OCH_2Ph)_2]\}_2$. The titanium *tert*-butoxide complex LTi(O^{t}Bu) reacts readily with dibenzyl phosphate to form a complex of the empirical formula $LTi[O_2P(OCH_2Ph)_2]$ (eq 3). In contrast to the complexes with apical ligands that form five- or six-membered chelate rings discussed above, the dibenzyl phosphate group does not chelate to the titanium. Instead, the dibenzyl phosphate groups bridge two LTi centers, forming a dimeric complex. The dimeric nature of the product is suggested by observation of a prominent peak at $m/z = 1986$ in the complex's FAB mass spectrum and is confirmed by X-ray crystallography (Figure 8).

The bond distances and angles in the complex are similar to the monomeric complexes, with the differential trans

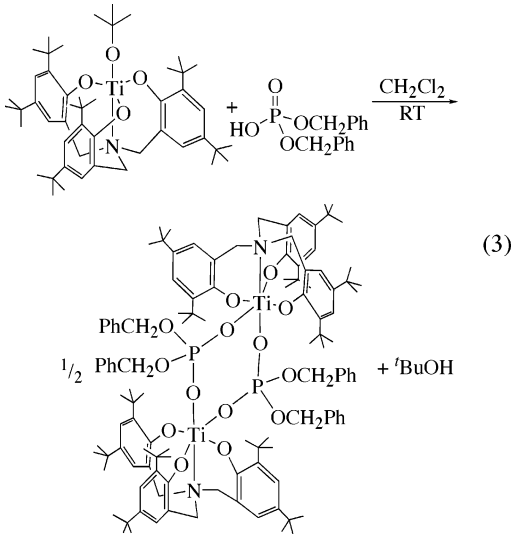

(3)

influence of the aryloxide and amine again differentiating the axial and equatorial titanium−phosphate bonds (1.964(3) vs 2.055(3) Å). The Ti−O−P angles are rather obtuse (165°), which may contribute to the preference for a bridged rather than a chelated structure, as may the need to form a four-membered ring to chelate. The acetate complex LTi(OAc) is monomeric and nonchelating in the solid state,[16] and the trifluoroacetate complex $LTi(O_2CCF_3)$ has also been inferred to be monodentate on the basis of IR spectroscopy.[11] The central eight-membered ring appears rather flat (rms deviation from the plane of 0.070 Å), but this may be due to unresolved disorder of the phosphate oxygen atoms between alternative puckered conformations, as suggested by the elongated thermal ellipsoids of O4 and O5. Early metal di-μ-phosphato complexes that are not further bridged by other ligands are generally puckered,[17] although the observation of widely varying conformations of the eight-membered ring in similar compounds suggests that the structure is rather flexible.[18]

One important difference between the phosphate-bridged dimer and the four monomeric complexes that have been characterized crystallographically is the conformation of the tripodal ligand. While the monomeric complexes all have a pseudo-C_3-symmetric conformation of the tripod, in the dibenzyl phosphate complex both of the aryloxides cis to the phosphates are folded back away from phosphate ligands, thus resembling the conformation shown by the octahedral tantalum complexes of nitrilotris(cresolate) ligands.[8] This difference in conformation is reflected in the NMR behavior of $\{LTi[O_2P(OCH_2Ph)_2]\}_2$, which shows time-average C_{2h} symmetry at all temperatures from −100 °C to room temperature. Thus, while the racemization of the ligand conformation can be frozen out in all of the bidentate chelates, it is rapid in $\{LTi[O_2P(OCH_2Ph)_2]\}_2$ at all temperatures examined, and while arm exchange is discernible in all of the bidentate complexes at or below room temperature, it is not observed in $\{LTi[O_2P(OCH_2Ph)_2]\}_2$.

Discussion

Mechanism of Ligand Racemization. The tripodal titanium alkoxide LTi(O^{t}Bu) reacts readily with tropolone,

(16) Fortner, K. C.; Brown, S. N., unpublished results.
(17) (a) Lugmair, C. G.; Tilley, T. D. *Inorg. Chem.* **1998**, *37*, 1821−1826. (b) Huang, C.-H.; Huang, L.-H.; Lii, K.-H. *Inorg. Chem.* **2001**, *40*, 2625−2627. (c) Dean, N. S.; Mokry, L. M.; Bond, M. R.; O'Connor, C. J.; Carrano, C. J. *Inorg. Chem.* **1996**, *35*, 2818−2825. (d) Chang, Y.-D.; Salta, J.; Zubieta, J. *Angew. Chem., Int. Ed. Engl.* **1994**, *33*, 325−327. (e) Chen, Q.; Salta, J.; Zubieta, J. *Inorg. Chem.* **1993**, *32*, 4485−4486.
(18) (a) Bond, M. R.; Mokry, L. M.; Otieno, T.; Thompson, J.; Carrano, C. J. *Inorg. Chem.* **1995**, *34*, 1894−1905. (b) Dean, N. S.; Bond, M. R.; O'Connor, C. J.; Carrano, C. J. *Inorg. Chem.* **1996**, *35*, 7643−7648.

Scheme 2. Schematic Mechanism of Ligand Racemization in Six-Coordinate Complexes[a]

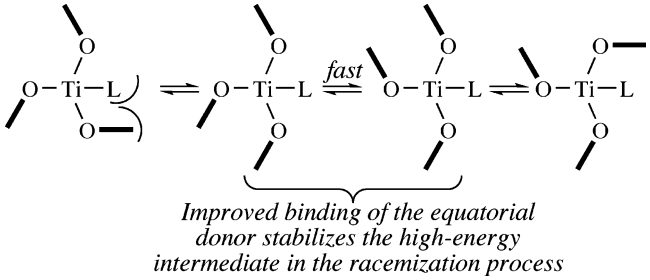

[a] Only the equatorial plane is shown.

β-diketones, 8-hydroxyquinoline, salicylaldehydes, and anthrarufin, with loss of *tert*-butyl alcohol and formation of six-coordinate complexes (eqs 1 and 2). In all cases, low-temperature NMR spectroscopy indicates that the tripodal ligand maintains the same pseudo-C_3-symmetric, propeller-like conformation observed in the trigonal bipyramidal complexes.[6−7,11] In five-coordinate LTi(O^{i}Pr), this conformation is rather resistant to racemization, with a barrier to twisting of 17.8 kcal/mol at 113 °C.[6] The six-coordinate complexes are markedly more mobile, with racemization taking place on the NMR time scale at temperatures below −60 °C in all cases. Even if the rates are extrapolated to 386 K, the six-coordinate complexes racemize from 10^3 to 10^5 times faster than the isopropoxide.

In contrast to the marked difference between the five- and six-coordinate complexes, the differences among the six-coordinate species are relatively slight. At −70 °C, where the rates can all be measured, all of the oxygen-ligated complexes racemize at rates clustered within a factor of 3 (between 170 and 540 s^{-1}). Only the hydroxyquinolinate complex falls out of this cluster, and even it racemizes only an order of magnitude more slowly (k_{rac} = 19 s^{-1} at −70 °C). Thus, while the presence of an equatorial ligand dramatically accelerates the flexing of the ligand backbone, its nature is of little importance.

One can conclude that the equatorial ligand binds much more tightly to the transition state for ligand flexing than to the ground state. In the ground state, one of the mutually trans aryloxide groups of the tripodal ligand points toward the equatorial ligand (O1 and its attendant aryl ring in the structures of the chelated complexes, Figures 1−4). Enhanced binding of the equatorial ligand might plausibly be due to an opening of the cleft where it binds when that arm flexes away (Scheme 2). This explanation requires that twisting the first arm is rate-determining and that the second arm flips back and forth rapidly in this high-energy conformation. The behavior of the μ-phosphato complex $\{LTi[O_2P(OCH_2Ph)_2]\}_2$ is consistent with this: in this species, the ligand adopts such an unsymmetrical geometry as its low-energy conformation, and even at −100 °C the tripodal ligand exhibits local C_s symmetry in the NMR, indicating that the central phenoxide arm is indeed rapidly flexing back and forth.

Mechanism of Ligand Arm Exchange. Unlike racemization, arm exchange is extremely sensitive to the nature of the chelating ligand, with the rates decreasing in the order tropolonate (too fast to measure at −100 °C) ≫ acac, 8-hydroxyquinolinate (3.8 and 2.0 × 10^2 s^{-1} at −50 °C, respectively) > salicylaldehyde (3.4 × 10^2 s^{-1} at −20 °C) ≫ anthrarufin, diformylcresolate, di-*p*-toluoylmethanide (3.9, 2.5, and 1.8 × 10^2 s^{-1} at 30 °C, respectively). This ordering shows no correlation with the electronic properties of the chelates, but does parallel their sizes. The five-membered chelates are both on the fast end of the scale, consistent with their lower steric profile as compared to the six-membered rings. The diformylcresolate complex and the anthrarufin complex are each more substituted on one end of the chelate as compared to the salicylaldehyde complex and show slowed arm interchange, while di-*p*-toluoylmethanide, which is extended on both ends as compared to acetylacetonate, imparts a markedly slower rate of arm exchange.

One plausible mechanism for arm interchange would involve dissociation of the neutral, equatorial donor of the bidentate chelate to form a C_3-symmetric, five-coordinate titanium complex. Three lines of evidence disfavor this mechanism. First, increasing the size of the bidentate ligand slows arm interchange rather than accelerating it as would be expected for a dissociative mechanism. Second, the observation that tripod arm exchange takes place concurrently with end-to-end exchange of the symmetrical bidentate ligands (tropolonate and the β-diketonates) is difficult to reconcile with this mechanism. If dissociation takes place equatorially, as expected given the pronounced trans influence observed in these complexes, then reassociation would (by microscopic reversibility) also take place equatorially, and tripod arm exchange would be expected to take place without scrambling the ends of the bidentate ligand. (Partial dissociation of β-diketonatotitanium(IV) complexes has been estimated to require ∼25 kcal/mol[19] and would thus be expected to be energetically inaccessible in any case.) Finally, ligand dissociation can be monitored independently in the diformylcresolate complex, and it takes place too slowly to account for the tripod arm exchange. While this is definitive only for the dfc complex, because this complex has one of the slowest rates of tripod arm exchange and is expected to have one of the more weakly bound equatorial ligands, the conclusion can reasonably be applied to most of the other complexes.

More compatible with the data is an intramolecular, twist-type mechanism (Scheme 1). Such interconversion of octahedral structures via trigonal prismatic geometry is very well precedented, having been documented in titanium(IV) bis(diketonate) complexes,[19,20] in zirconium(IV) diketiminates,[21] and in a zirconium(IV) complex of a dianionic tripod.[22] The geometric constraints of the tripod limit the possible trigonal prisms to two essentially enantiomorphous structures,[23] corresponding to whether the bidentate group

(19) Baggett, N.; Poolton, D. S. P.; Jennings, W. B. *J. Chem. Soc., Dalton Trans.* **1979**, 1128−1134.
(20) Fay, R. C.; Lindmark, A. F. *J. Am. Chem. Soc.* **1983**, *105*, 2118−2127.
(21) Rahim, M.; Taylor, N. J.; Xin, S.; Collins, S. *Organometallics* **1998**, *17*, 1315−1323.
(22) Toupance, T.; Dubberley, S. R.; Rees, N. H.; Tyrrell, B. R.; Mountford, P. *Organometallics* **2002**, *21*, 1367−1382.

migrates to the cleft on its right or the one on its left. Passage through such a structure explains why tripod arm exchange and exchange of the ends of symmetrical bidentate ligands occur at the same time. It also explains why increasing bulk on either end of the bidentate ligand has a similar decelerating effect on the arm exchange (compare $[LTi]_2$[anruf] or LTi[dfc] to LTi[sal]). In the octahedral complex, the apical end of the chelate is in the center of the flanking *tert*-butyl groups of the tripod and the equatorial end is below them, while in the intermediate geometry both ends are in similar contact with the bulky periphery of the tripod.

The symmetry of this system also allows one to address a subtle point about this mechanism that has not previously been amenable to study. In the intermediate geometry, the tripod has approximately regained its three-fold axis, which is now more or less coincident with the two-fold (or pseudo-two-fold) axis of the bidentate ligand. If this structure were a true intermediate, with a significant lifetime, then one would expect facile rotation of the two fragments about the common axis, leading to interconversion of the structures with the bidentate ligand intercalated in the three possible clefts, and with either end of the bidentate ligand facing the clefts (Scheme 1b). Conversely, if the nonoctahedral structure were a transition state, then the motion of the bidentate ligand would be "ballistic", with the bidentate ligand doing an uninterrupted flip between clefts (Scheme 1a). The experimental data (Figure 7) clearly support the latter mechanism.

These results indicate that the trigonal prismatic geometry in this system most likely represents the energy maximum of a transition state, although a lifetime for this geometry that is finite but too short to permit swiveling of the bidentate ligand relative to the tripod cannot be ruled out. While trigonal prismatic titanium(IV) complexes are known,[24] they are rare. The facile geometric interconversions of many octahedral Ti(IV) complexes imply that prismatic geometries are energetically accessible. The present study provides the first evidence that these structures are likely to be maxima, rather than long-lived alternative structures, on the potential energy surfaces of many six-coordinate titanium(IV) complexes.

(23) Technically, because the tripodal arms are folded to the right or to the left, the two possible trigonal prisms are diastereomers and the two directions of bidentate ligand migration are inequivalent. However, because counterclockwise and clockwise rotation are the reverse of each other, and because the equilibrium constant for this degenerate reaction is unity, microscopic reversibility requires that rotation in the two directions must take place at equal rates. For discussion of an analogous situation in an organic rotor, see: Kelly, T. R.; Sestelo, J. P.; Tellitu, I. *J. Org. Chem.* **1998**, *63*, 3655−3665.

(24) (a) Steinhuebel, D. P.; Lippard, S. J. *Inorg. Chem.* **1999**, *38*, 6225−6233. (b) Goedken, V. L.; Ladd, J. A. *J. Chem. Soc., Chem. Commun.* **1982**, 142−144. (c) Blake, A. J.; McInnes, J. M.; Mountford, P.; Nikonov, G. I.; Swallow, D.; Watkin, D. J. *J. Chem. Soc., Dalton Trans.* **1999**, 379−391. (d) Housemekerides, C. E.; Ramage, D. L.; Kretz, C. M.; Shontz, J. T.; Pilato, R. S.; Geoffroy, G. L.; Rheingold, A. L.; Haggerty, B. S. *Inorg. Chem.* **1992**, *31*, 4453−4468.

Conclusions

The aminetris(phenoxide)titanium(IV) *tert*-butoxide complex $[N(CH_2C_6H_2\text{-}3,5\text{-}{}^tBu_2\text{-}2\text{-}O)_3]Ti(O{}^tBu)$ ($LTiO{}^tBu$) reacts readily with the protonated forms of bidentate, monoanionic ligands to form octahedral, six-coordinate complexes. Chelates that form five- or six-membered rings form monomeric complexes, while dibenzyl phosphate forms a phosphate-bridged dimer. Six-coordination is readily achieved in the presence of the tripodal ligand, with a substantial barrier to dissociation of the sixth ligand in the one case in which it has been observed ($\Delta H^{\ddagger} = 17.0$ kcal/mol for dissociation of the bound aldehyde in the 2,6-diformyl-*p*-cresolate complex). The tripodal ligand in the monomeric complexes displays a propeller-like conformation, with inversion of the helical sense of the conformation taking place much more rapidly than in the five-coordinate $LTi(O{}^iPr)$. This twisting process is relatively insensitive to the sterics or electronics of the bidentate ligand and occurs in a stepwise fashion rather than involving concurrent twisting of all three arms. Motion of the bidentate ligand between clefts in the tripod, which exchanges the phenoxide arms cis and trans to the equatorial donor of the bidentate ligand, also takes place readily, with rates that increase as the steric profile of the bidentate ligand decreases. Arm exchange takes place predominantly by a nondissociative twist mechanism. The nonoctahedral geometry that mediates the exchange appears to have too short a lifetime to allow the bidentate ligand to reorient itself during its passage.

Acknowledgment. We thank Dr. Alicia Beatty for assistance with the X-ray crystallography. Financial support of this work by the University of Notre Dame and BLURP is gratefully acknowledged.

Supporting Information Available: Variable-temperature ^1H NMR spectra of LTi(trop), and Eyring plots for ligand racemization rates, arm exchange rates, and aldehyde exchange rate constants; crystallographic data for LTi(trop), LTi(acac), LTi(hq)·CH_3CN·$0.5C_6H_6$, LTi(dfc)·CH_2Cl_2, and $\{LTi[O_2P(OCH_2Ph)_2]_2\}_2$·$4CH_2Cl_2$ in CIF format. This material is available free of charge via the Internet at http://pubs.acs.org.

IC048403D